Eur. Phys. J. B **13**, 41–45 (2000)

THE EUROPEAN PHYSICAL JOURNAL B

EDP Sciences

Enhancement of magnetoresistance in cobaltites by manganese substitution: the oxide $La_{0.8}Sr_{0.2}Co_{1-x}Mn_xO_3$

A. Maignan[a], C. Martin, M. Hervieu, and B. Raveau

Laboratoire CRISMAT[b], ISMRA et Université de Caen, 6 Boulevard du Maréchal Juin, 14050 Caen Cedex, France

Received 7 May 1999

Abstract. The substitution of manganese for cobalt in the perovskite $La_{0.8}Sr_{0.2}CoO_3$ has been studied. A significant increase of the magnetoresistance (MR) is obtained, $MR = -100(\rho_H - \rho_0)/\rho_0$ reaching 60% at 5 K under 7 T for $x \cong 0.10$. This behavior originates from a spectacular increase of the resistivity correlated to a significant decrease of ferromagnetism by Mn doping. This enhancement of magnetoresistance can be interpreted by the growth of ferromagnetic clusters in the insulating matrix, by applying a magnetic field.

PACS. 71.30.+h Metal-insulator transitions and other electronic transitions – 75.70.Pa Giant magnetoresistance

1 Introduction

The discovery of large magnetoresistance (MR) in the perovskites $La_{1-x}Sr_xCoO_3$ by Briceno *et al.* [1] makes this system attractive for magnetic investigations, in spite of the fact that the resistance ratio ρ_0/ρ_{6T} remains small [2–5], *i.e.* inferior to 2, compared to the values obtained for the manganites which reach several orders of magnitude [6–11].

The similarity between the cobaltites and manganites lies in the fact that both of them exhibit a ferromagnetic metallic (FMM) state by creation of holes, *i.e.* by introducing Mn^{4+} or Co^{4+} species in a Mn^{3+} or Co^{3+} matrix. Nevertheless, the origin of the magnetoresistance effect in the two series of oxides is fundamentally different. The colossal magnetoresistance properties of manganites are governed by double exchange phenomena [12,13], *i.e.* by double exchange Mn^{3+}–O–Mn^{4+} interactions as Mn^{4+} species are introduced in the Mn^{3+} matrix *via* the La^{3+}/Sr^{2+} substitution. In contrast to the high-spin configuration of Mn^{3+} and Mn^{4+}, the spin-state of trivalent or tetravalent cobalt depends on temperature [14–16]. In particular, $LaCoO_3$ exhibits two spin-state transitions, as T increases from liquid helium temperature, from low-spin (LS) to intermediate-spin (IS) and then from IS to high-spin (HS). As shown experimentally [16], the creation of Co^{4+} cations in the Co^{3+} matrix of $LaCoO_3$ by the Sr^{2+} for La^{3+} substitution changes the LS state observed at low temperature (susceptibility (χ) ~ 0) in a more magnetic state ($\chi \gg 0$). Consequently it has been proposed, that the Sr^{2+} substitution leads to the formation of IS ferromagnetic clusters, stabilized even for the lowest temperatures. Each cluster would consist of one — or several — Co^{4+} (LS) surrounded by IS-Co^{3+} cations with ferromagnetic interactions Co^{4+}–O–Co^{3+}. Thus, the insulator-metal (I-M) transition in $La_{1-x}Sr_xCoO_3$ would result from the creation of a percolative path between the growing ferromagnetic clusters. In this respect, the growth of clusters would be also favored by the application of a magnetic field, leading to the negative magnetoresistance [2,17]. This assumption is confirmed by the observation of a MR maximum for compositions lying in the vicinity of the I-M transition, *i.e.* x values of 0.1–0.2.

These results suggest that, starting from the composition $La_{0.8}Sr_{0.2}CoO_3$, which exhibits a cobalt (IV) content adequate for the I-M transition, with a FMM state below T_C, it should be possible to enhance the MR properties of this material, by changing the size of the FM clusters. In this respect, the doping of the cobalt sites by other magnetic cations may be of great interest. This viewpoint is supported by the recent announcement of giant magnetoresistance in $La_{0.8}Sr_{0.2}Co_{1-x}Fe_xO_3$ for $x \cong 0.025$ [18]. A MR ratio of 90% under 7.5 T at 300 K was indeed found for this Fe-doped cobaltite. Unfortunately, this result was not confirmed by other authors and we were not able to reproduce this observation.

The ability of manganese to adopt the same mixed valence as cobalt, *i.e.* Mn^{3+}–Mn^{4+}, and the evidence for ferromagnetic coupling between Mn^{3+} and Co^{3+}, shown by Jonker [19] for $LaCo_{1-x}Mn_xO_3$, suggest the possibility to modify significantly the transport and magnetic properties of $La_{0.8}Sr_{0.2}CoO_3$ by manganese doping. In the present letter, we show that the unconventional ferromagnetism of $La_{0.8}Sr_{0.2}CoO_3$ can be dramatically weakened by Mn doping, leading to a significant increase of magnetoresistance with respect to the pristine compound.

[a] e-mail: antoine.maignan@ismra.fr
[b] UMR 6508 associée au CNRS

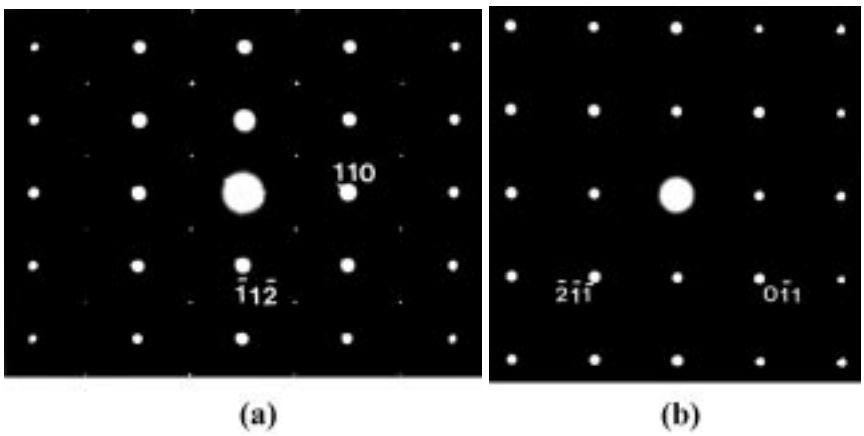

Fig. 1. $La_{0.8}Sr_{0.2}Co_{0.9}Mn_{0.1}O_3$: (a) $[\bar{2}01]_H$ and (b) $[1\bar{1}1]_H$ electron diffraction patterns.

Sintered pellets of $La_{0.8}Sr_{0.2}Co_{1-x}Mn_xO_3$ were prepared according to the classical procedure, heating mixtures of La_2O_3, $SrCO_3$, Co_3O_4 and MnO_2 in O_2 flow at 1 150 °C during 24 h. The X-ray patterns recorded for $La_{0.8}Sr_{0.2}Co_{1-x}Mn_xO_3$, with $x = 0$ and 0.1, show single phased perovskite type samples. The cell parameters have been refined (using the Fullprof program) in the $R\bar{3}c$ space group previously reported for this kind of compounds [20], leading to ($a = 5.443\,1(2)$ Å, $c = 13.182(1)$ Å) for $x = 0$ and (5.442 8(1) Å, 13.186(1) Å) for $x = 0.1$. The oxygen content, determined by iodometric titration, was found to be 3.00 in the error of the technique estimated to ±0.02 for all the investigated samples ($0 \leq x \leq 0.10$).

The electron microscopy characterisation was carried out for both undoped, $La_{0.8}Sr_{0.2}CoO_3$, and Mn doped $La_{0.8}Sr_{0.2}Co_{0.9}Mn_{0.1}O_3$, compounds. The crystallites in suspension in alcohol were deposited onto a holey carbon film supported by a copper grid. The electron diffraction (ED) study was carried out with a JEOL 200CX electron microscope. Numerous crystallites of every sample were characterised by reconstructing the reciprocal space, tilting around the crystallographic axes and by combining energy dispersive spectroscopy (EDS) analyses.

The EDS analyses showed the homogeneity of both samples, the different grains exhibiting, in the limit of accuracy of the technique, actual compositions very close to the nominal ones, *i.e.* $La_{0.8}Sr_{0.2}Co$ and $La_{0.8}Sr_{0.2}Co_{0.9}Mn_{0.1}$ cationic ratios.

Despite the two samples followed exactly the same thermal synthesis process, a significant difference in the crystal habitus was observed. The crystallites of the undoped $La_{0.8}Sr_{0.2}CoO_3$ are small, a few hundred nanometers maximum thick, and often exhibit strain effects whereas the $La_{0.8}Sr_{0.2}Co_{0.9}Mn_{0.1}O_3$ flakes are considerably larger (at least one order of magnitude), and exhibit a high degree of crystallinity.

The ED investigation shows that the system of the intense Bragg reflections is consistent with the rhombohedral lattice, $R\bar{3}c$ space group, previously proposed [20]. However, for the $La_{0.8}Sr_{0.2}CoO_3$ cobaltite, the reflections often exhibit elongated shapes, correlated to tweed phenomena which are supposed to be, at least, partly responsible for the strain effects, and long exposures of the patterns show that the actual symmetry is likely lowered. These effects are almost no more visible in $La_{0.8}Sr_{0.2}Co_{0.9}Mn_{0.1}O_3$. This is illustrated in Figure 1, which presents the $[\bar{2}01]_H$ and $[\bar{1}11]_H$ patterns (hexagonal indexation), which correspond to the $[101]_P$ and $[100]_P$ pattern of the cubic perovskite subcell.

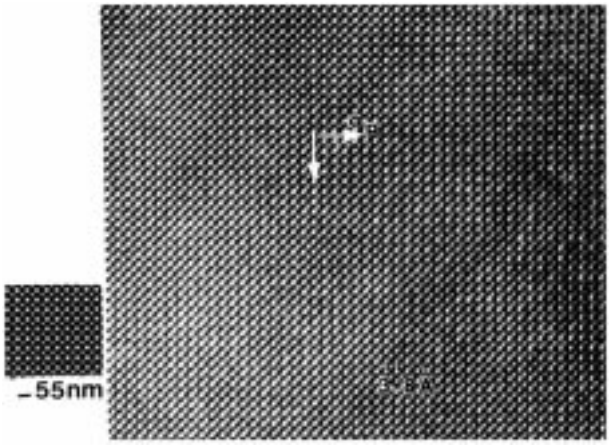

Fig. 2. $[\bar{2}01]_H$ HREM image of the Mn 10% doped cobaltite. It corresponds to a $[001]_p$ viewing direction of the perovskite subcell (indicated by a_p). The bright dots are correlated to the cation positions.

The high resolution electron microscopy (HREM) was carried out with a TOPCON 002B microscope (200 kV and $C_s = 0.4$ mm), also equipped with an EDS analyser. HREM images calculations were carried out with the Mac-Tempas multislice program. The $[100]_H$, $[110]_H$ $[\bar{1}11]_H$, $[\bar{2}01]_H$ and $[001]_H$ viewing directions have been selected. The HREM images of $La_{0.8}Sr_{0.2}Co_{0.9}Mn_{0.1}O_3$ exhibit a very regular contrast. One example of $[\bar{2}01]_H$ image is given in Figure 2, where the cationic positions are highlighted; it is compared with the corresponding theoretical image, calculated from the refined positional parameters. The different images show that there is no extended defect

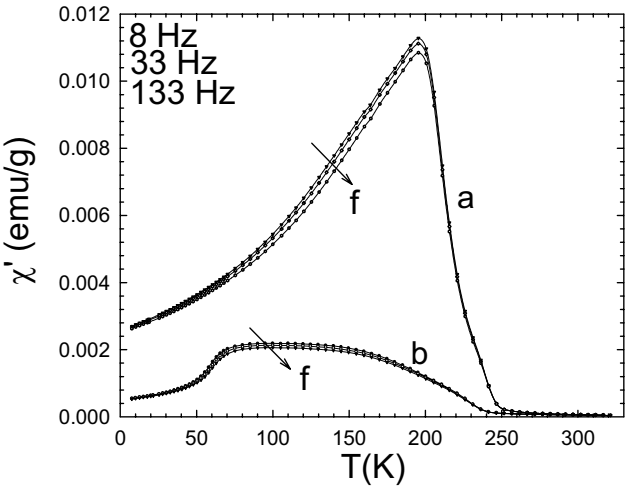

Fig. 3. Real-part of the AC-susceptibility (χ') registered with h_{ac} = 10 Oe (frequencies are labelled on the graph). (a) $La_{0.8}Sr_{0.2}CoO_3$, (b) $La_{0.8}Sr_{0.2}Co_{0.9}Mn_{0.1}O_3$.

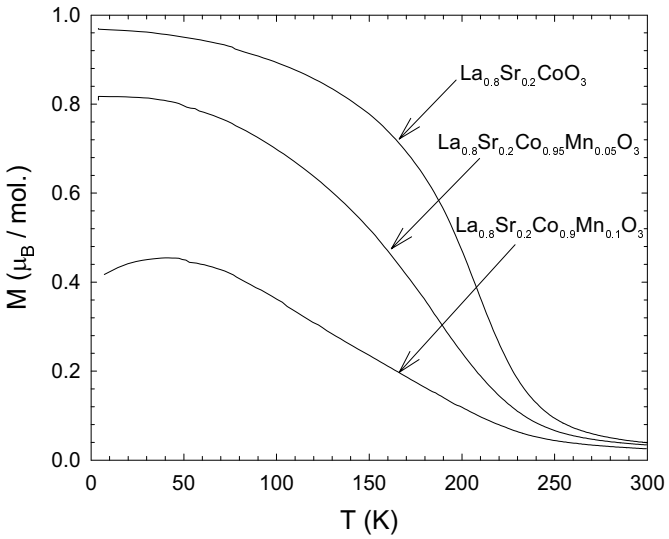

Fig. 4. T dependent magnetization registered upon heating in 1.45 T after a zero-field- cooling.

nor local order-disorder phenomena which systematically take place in these crystallites and which could influence the physical properties. In particular, for both samples $x = 0$ and 0.1, we did not detect any phenomenon which could indicate an inhomogeneous local distribution of La-rich and Sr-rich planes, contrary to what was observed in the $La_{0.7}Sr_{0.3}CoO_3$ cobaltite [20].

The ac-susceptibility curve of $La_{0.8}Sr_{0.2}CoO_3$ (Fig. 3) shows a broad FM transition peaking at 200 K. This is consistent with a cluster glass behavior rather than a conventional FM one, in agreement with previous observations [3,16]. The substitution of Mn for Co in $La_{0.8}Sr_{0.2}CoO_3$ tends to reduce the FM state of the sample as shown from the ac-χ curve of $La_{0.8}Sr_{0.2}Co_{0.9}Mn_{0.1}O_3$ (Fig. 3). Though χ' also starts to increase below 240 K, the shape of the curve becomes rather flat on the maximum region with χ' values strongly reduced in comparison with $La_{0.8}Sr_{0.2}CoO_3$. Such a curve shape is usually encountered for $La_{0.9}Sr_{0.1}CoO_3$ which indicates that the Mn for Co substitution tends to strongly reduce the FM state in contrast with the expected FM coupling between Mn^{3+} and Co^{3+} proposed by Jonker [19]. The decrease of the FM interactions is also shown from the magnetization curves (Fig. 4). The magnetic moment at 4 K decreases indeed from 1 μB per Co mol for $La_{0.8}Sr_{0.2}CoO_3$ to 0.4 μ_B for $La_{0.8}Sr_{0.2}Co_{0.9}Mn_{0.1}O_3$. The magnetic properties similarity between $La_{0.8}Sr_{0.2}Co_{0.9}Mn_{0.1}O_3$ and $La_{0.9}Sr_{0.1}CoO_3$ strongly suggests that the Mn for Co substitution reduces the FM clusters size, which decreases as x decreases in $La_{1-x}Sr_xCoO_3$ [2]. This may indicate that in $La_{0.8}Sr_{0.2}Co_{0.9}Mn_{0.1}O_3$, the holes would be preferentially created as Mn^{4+} rather than Co^{4+}. In this case, the size of the FM clusters, stabilized by the presence of Co^{4+}, would be reduced.

The transport properties are also significantly modified by Mn doping as shown from the $\rho(T)$ curves (Fig. 5). The pristine phase $La_{0.8}Sr_{0.2}CoO_3$ is indeed metallic, with a metal-metal transition around 210 K (Fig. 5a), *i.e.* below T_C deduced from the $\chi'(T)$ curve (Fig. 3). In contrast, the Mn doped samples are semiconductors like as shown for 10% Mn (Fig. 5b), the low temperature resistivity increasing by several orders of magnitude, as shown by the ρ values at 10 K which range from 3×10^{-4} Ωcm for $La_{0.8}Sr_{0.2}CoO_3$ (Fig. 5a) to 10^3 Ωcm $La_{0.8}Sr_{0.2}Co_{0.9}Mn_{0.1}O_3$ (Fig. 5b). At room temperature the Mn for Co substitution also induces an increase of the resistivity (Fig. 5) correlated with the decrease of the size of the FM clusters (Fig. 4). This result is consistent with the previous assumption of holes creation mainly as Mn^{4+} species. In that case, the reduction of the FM clusters size, induced by the Mn^{4+} for Co^{4+} substitution, would tend to make the resistivity increase.

The magnetoresistance is then correlated to the variation of magnetic and transport properties by Mn doping. In the pristine compound, the $\rho(T)$ curve registered under 7 T (Fig. 5a) shows a negative MR effect, which is maximum at the metal-metal transition temperature (210 K). This suggests that MR originates from a better coupling between FM clusters by applying a magnetic field. In contrast, in the Mn-doped cobaltite, MR is very weak (~ 0) close to T_C (Fig. 5b), but increases as T decreases, reaching much higher resistance ratio than for the pristine phase below T_C, *i.e.* $\rho_0/\rho_{7T} \cong 4.5$ at 5 K for 10% Mn doping against $\cong 1.07$ at 210 K without Mn (Fig. 5b). This situation, where the maximum of magnetoresistance is displaced from T_C toward lower temperatures by Mn doping, is similar to what is observed by decreasing the hole concentration in $La_{1-x}Sr_xCoO_3$, as shown for instance by comparing the $\rho(T)$ curves of $La_{0.8}Sr_{0.2}CoO_3$ (Fig. 5a) and of $La_{0.93}Sr_{0.07}CoO_3$ (Fig. 5c). Thus, it seems reasonable to assume that the manganese doping, in the form of Mn^{4+} cations in $La_{0.8}Sr_{0.2}CoO_3$, tends to reduce the number of Co^{4+} which are believed to be the mobile holes in the FM clusters. However, additional local techniques

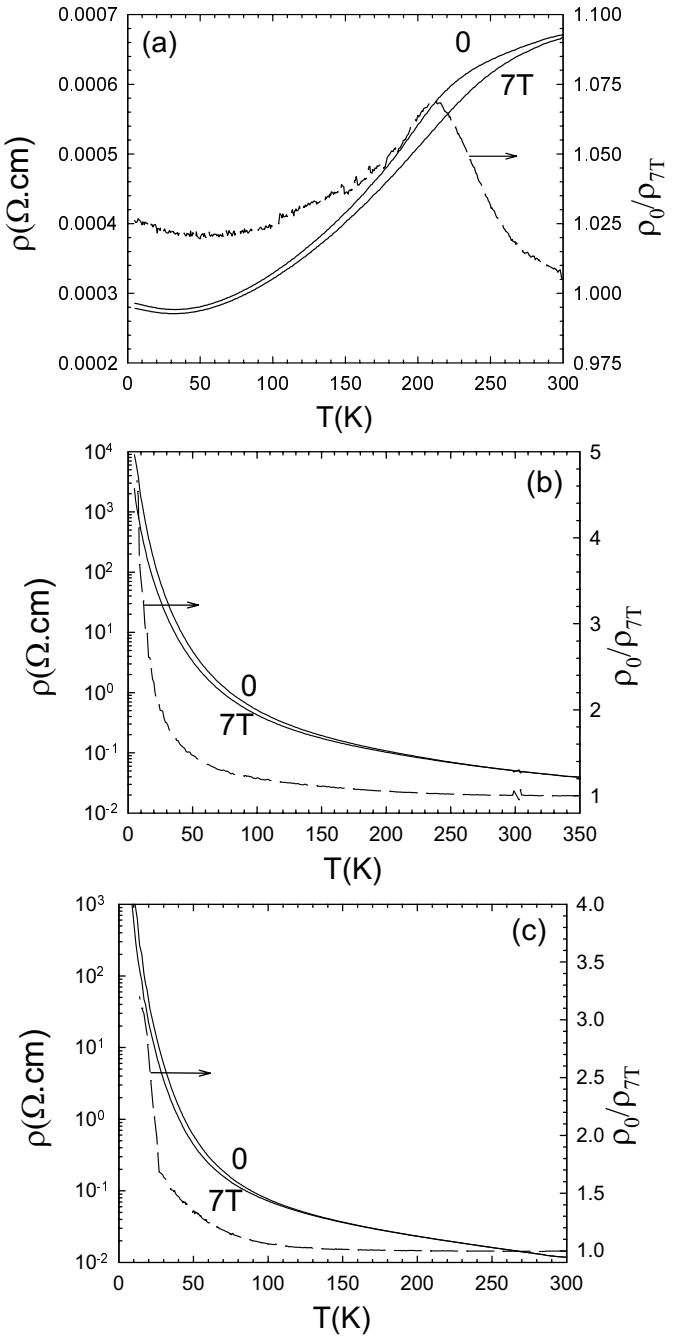

Fig. 5. T dependent resistivity curves registered upon cooling in 0 and 7 T. The ρ_0/ρ_{7T} ratio is also given (dashed line, right y-axis). (a) $La_{0.8}Sr_{0.2}CoO_3$, (b) $La_{0.8}Sr_{0.2}Co_{0.90}Mn_{0.10}O_3$ and (c) $La_{0.93}Sr_{0.07}CoO_3$.

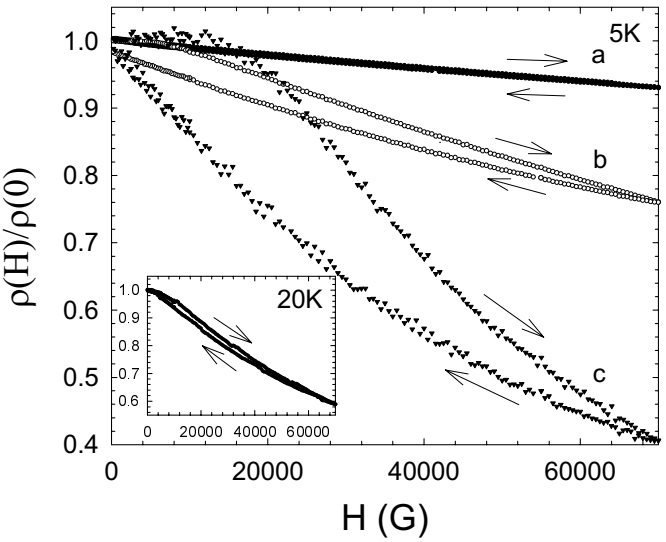

Fig. 6. Field (H) dependent normalized resistivities $\rho(H)/\rho(0)$ registered at 5 K. (a) $La_{0.8}Sr_{0.2}CoO_3$, (b) $La_{0.8}Sr_{0.2}Co_{0.95}Mn_{0.05}O_3$, and (c) $La_{0.8}Sr_{0.2}Co_{0.9}Mn_{0.1}O_3$. Inset: normalized resistivity *versus* H for $La_{0.93}Sr_{0.07}CoO_3$ recorded at 20 K (the 5 K resistivity was too high to be measured).

as nuclear magnetic resonance (N.M.R.) should be used in order to confirm the preferential formation of Mn^{4+} species in $La_{0.8}Sr_{0.2}Co_{1-x}Mn_xO_3$.

Nevertheless, the isothermal magnetic field dependent $\rho(H)$ curves (Fig. 6) clearly demonstrate that the situation is not so simple. The Mn doped cobaltite $La_{0.8}Sr_{0.2}Co_{1-x}Mn_xO_3$ exhibits a larger MR effect than the pristine compound, the maximum MR increasing from 7% for $x = 0$ to 60% at 5 K for $x = 0.10$, through 25% at 20 K for $x = 0.05$. Moreover, the value obtained for 10% of Mn (60% in 7 T) is even better than that obtained for $La_{0.93}Sr_{0.07}CoO_3$ which exhibits the best MR properties of the $La_{1-x}Sr_xCoO_3$ series with 40% at 20 K in 7 T (Inset of Fig. 6) in good agreement with previous studies [2].

In conclusion, the doping of the cobalt sites in the $La_{0.8}Sr_{0.2}CoO_3$ oxide by manganese shows a spectacular transition from a metallic to an insulating behavior correlated with a decrease of the unconventional ferromagnetism in this compound. It is thus the growth of the FM metallic clusters under a magnetic field, in the insulating matrix, which is at the origin of the larger MR effect observed at low temperature for Mn-doped compounds. The present results may be understood if the mobile holes creation in the form of Co^{4+} in FM clusters, induced by the La^{3+}/Sr^{2+} substitution, are progressively replaced by localized Mn^{4+} species in $La_{0.8}Sr_{0.2}Co_{1-x}Mn_xO_3$.

References

1. G. Briceno, H. Chang, X. Sun, P.G. Schultz, X.D. Xiang, Science **270**, 273 (1995).
2. R. Mahendiran, A.K. Raychaudhuri, Phys. Rev. B **54**, 16044 (1996).
3. S. Yamaguchi, H. Taniguchi, H. Takagi, T. Arima, Y. Tokura, J. Phys. Soc. Jap. **64**, 1885 (1995).
4. V. Golovanov, L. Mihaly, A.R. Moodenbaugh, Phys. Rev. B **53**, 8207 (1996).
5. M.R. Ibarra, M. Mahendiran, C. Marquina, B. Garcia-Landa, J. Blasco, Phys. Rev. **57**, R3217 (1998).

6. R. von Helmolt, J. Wecker, B. Holzapfel, L. Schultz, K. Samwer, Phys. Rev. Lett. **71**, 2331 (1993).
7. G. Kido, N. Furukawa, J. Phys. Soc. Jap. **63**, 3931 (1994).
8. Y. Tokura, A. Urishibara, Y. Moritomo, T. Arima, A. Asamitsu, G. Kido, F. Furukawa, J. Phys. Soc. Jap. **63**, 3931 (1994).
9. K. Chahara, T. Ohno, M. Kasai, Y. Kozono, Appl. Phys. Lett. **63**, 1990 (1993).
10. H.L. Ju, C. Kwon, Q. Li, R.L. Greene, T. Venkatesan, Appl. Phys. Lett. **65**, 2108 (1994).
11. A. Maignan, Ch. Simon, V. Caignaert, B. Raveau, Solid St. Commun. **96**, 623 (1995).
12. C. Zener, Phys. Rev. **82**, 403 (1951).
13. P.G. de Gennes, Phys. Rev. **118**, 141 (1960).
14. P.M. Raccah, J.B. Goodenough, Phys. Rev. **155**, 932 (1967).
15. J.B. Goodenough, Mater. Res. Bull. **6**, 967 (1971).
16. M.A. Senaris-Rodriguez, J.B. Goodenough, J. Solid State Chem. **116**, 224 (1995); *ibid.* **118**, 323 (1995).
17. R. Mahendiran, A.K. Raychaudhuri, A. Chains, B.D. Sarma, J. Phys. Cond. Matter **7**, L561 (1995).
18. A. Barman, M. Gosh, S. Biswas, S.K. De, S. Chatterjee, Appl. Phys. Lett. **71**, 3150 (1997).
19. G.H. Jonker, J.H. van Santen, Physica **16**, 337 (1950).
20. R. Caciuffo, D. Rinaldi, G. Barucca, J. Mira, J. Rivas, M.A. Senaris-Rodriguez, P.G. Radaelli, D. Fiorani, J.B. Goodenough, Phys. Rev. B **59**, 1068 (1999).